DOI: 10.1002/

Article type: *Research News*

Functionalization of Two-Dimensional Transition Metal Dichalcogenides

*Xin Chen, Aidan R. McDonald**

Ms. Xin Chen, Dr. Aidan R. McDonald,

School of Chemistry and CRANN/AMBER Nanoscience Institute,

Trinity College Dublin, The University of Dublin,

College Green, Dublin 2,

Ireland.

email: aidan.mcdonald@tcd.ie

Abstract

Two-dimensional (2D) layered transition metal dichalcogenides (TMDs) are a fascinating class of nanomaterials that have the potential for application in catalysis, electronics, photonics, energy storage, and sensing. TMDs are rather inert, and thus pose problems for chemical derivatization. However, to further modify the properties of TMDs and fully harness their capabilities, routes towards their chemical functionalization must be identified. In this research news article we critically review recent efforts towards the chemical (bond-forming) functionalization of 2D TMDs. We highlight recent successes and also areas where further detailed analyses and experimentation are required. As detailed herein, this burgeoning field is very much in its infancy but has already provided several important breakthroughs.

Graphical Abstract

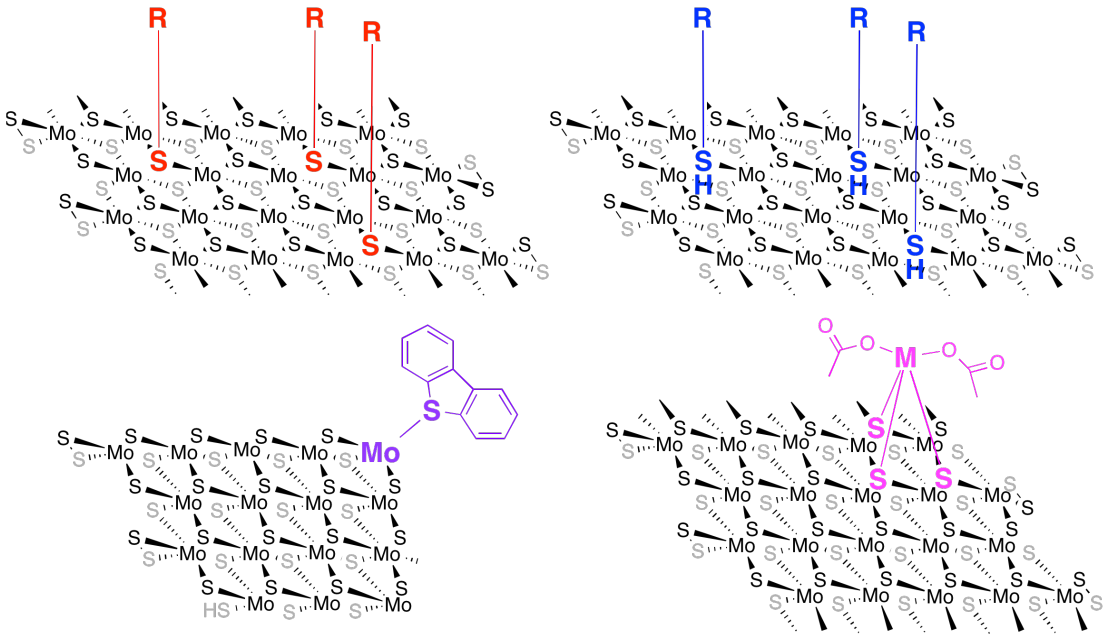

1. Introduction

Since the discovery of the extraordinary properties of graphene,[1-5] other two-dimensional (2D) nanomaterials, and in particular the layered transition metal dichalcogenides (TMDs), have garnered great interest.[6-11] This is due to their exciting physical and chemical properties. TMDs have been deemed suitable (and in some cases game-changing) for potential applications in a variety of areas (catalysis, electronics, photonics, energy storage, and sensing). Layered TMDs are a class of materials with MX_2 stoichiometry, where M refers to a transition metal typically from Groups 4-7 (M = Ti, Nb, Ta, Mo, W) of the periodic table and X refers to a chalcogen such as S, Se or Te. Approximately 40 different layered TMDs have been identified to date. Bulk 3D crystalline TMDs are stacked structures with strong covalent bonding between metal and chalcogen, and weak Van der Waals interactions between adjacent layers of MX_2 (Figure 1). These weak forces allow for the simple delamination of 3D crystals into 2D nanosheets through exfoliation. Each individual layer of TMDs exists in a polymeric X-M-X form, with a plane of transition metal atoms sandwiched between two planes of chalcogen atoms (Figure 1). Delaminated or exfoliated monolayers thus display a surface full of chalcogen atoms with the metal atoms embedded within the monolayer.

2D TMDs exhibit disparate electronic structures either as a result of electronic configuration (*d*-electron count, thus metal and oxidation state determine electronic configuration) or the coordination environment of the transition metal.[12] The coordination of metal atoms in layered TMDs is most often found to be either octahedral (1T polymorph) or trigonal prismatic (2H polymorph) (Figure 1). TMDs with metals in an octahedral coordination environment (D_{3d}) display a unique *d*-

orbital splitting (d_z^2, $d_{x^2-y^2}$ (e_g) and $d_{yz,xz,xy}$ (t_{2g})), whereas TMDs with metals in a trigonal prismatic coordination environment (D_{3h}) obviously show a different d-orbital splitting (d_z^2 (a1), $d_{x^2-y^2}$, d_{xy} (e), and $d_{xz,yz}$ (e′)).[12-15] These differences in *d*-orbital splitting cause the polymorphs to display quite different physical properties, even for materials containing the same MX_2 elemental formula. For example, monolayers of 1T-MoS_2 are metallic, whereas monolayers of 2H-MoS_2 are semi-conducting with a sizeable band gap (~1.2 eV).

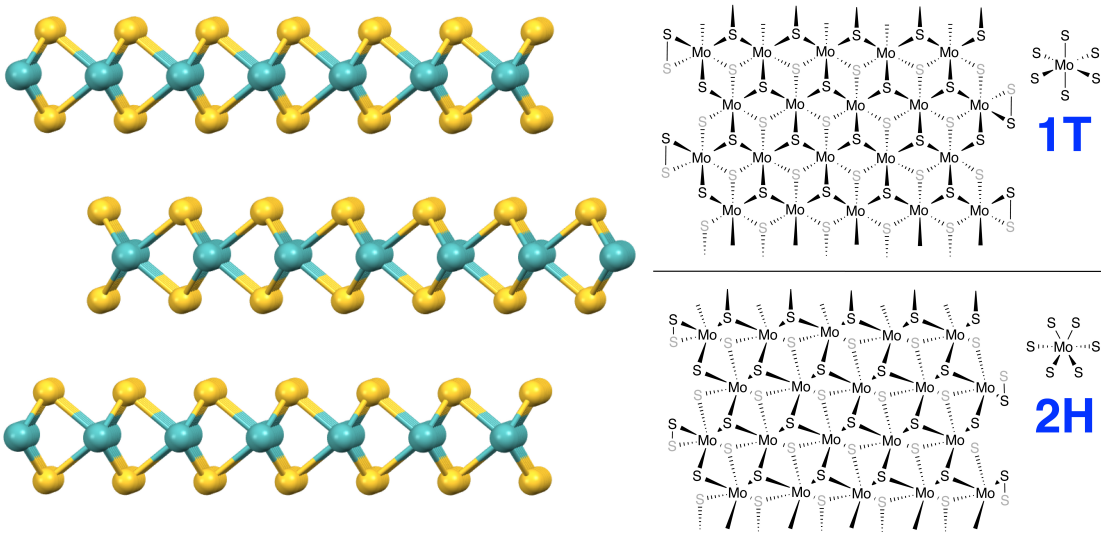

Figure 1. Left: side-on view of packing diagram for 2H-MoS_2 (yellow spheres = S-atoms; cyan spheres = Mo-atoms).[16] Right: top-down view of ChemDraw representation of 1T-MoS_2 (top) and 2H-MoS_2 (bottom).

A major focus of experimental research in recent years has concentrated on the development of experimental methods to produce high-quality TMD nanosheets. The commonly applied techniques include mechanical cleavage, solution-based exfoliation, Chemical Vapor Deposition (CVD), and hydrothermal synthesis.[7, 17-22] These strategies for TMD nanosheet production allow for deep investigation of their layer-dependent properties, and investigations into their future industrial application.

To further modify their properties, fully harness their capabilities, and even broaden their application, chemical functionalization of such layered TMD materials is an absolute necessity.[23] Unfortunately, TMDs tend to be rather inert to chemical functionalization. Chalcogen atoms in the basal plane of TMD nanosheets are saturated and thus are not highly reactive (Figure 1), while the metal sites in TMDs are embedded beneath the chalcogen layer, all but eliminating them from being useful for functionalization. Herein, we review recent synthetic efforts towards the chemical functionalization of two-dimensional TMDs. Most efforts to date have focused on MoS_2, the prototypical TMD, and both isolable polymorphs of MoS_2 (1T- and 2H-) have attracted equal attention. We have focused solely on efforts to perform chemical functionalization (i.e. bond formation between functionality and TMD), and have not covered reports into the functionalization of TMDs through physisorption or non-bond forming methods.[24-31]

2. Functionalization of 1T-MoS_2

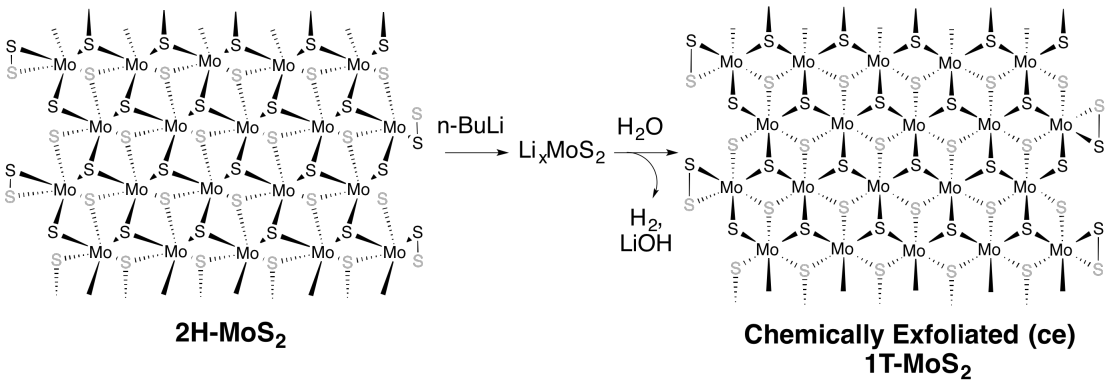

Scheme 1. Preparation of ce-1T-MoS_2 from bulk 2H-MoS_2.

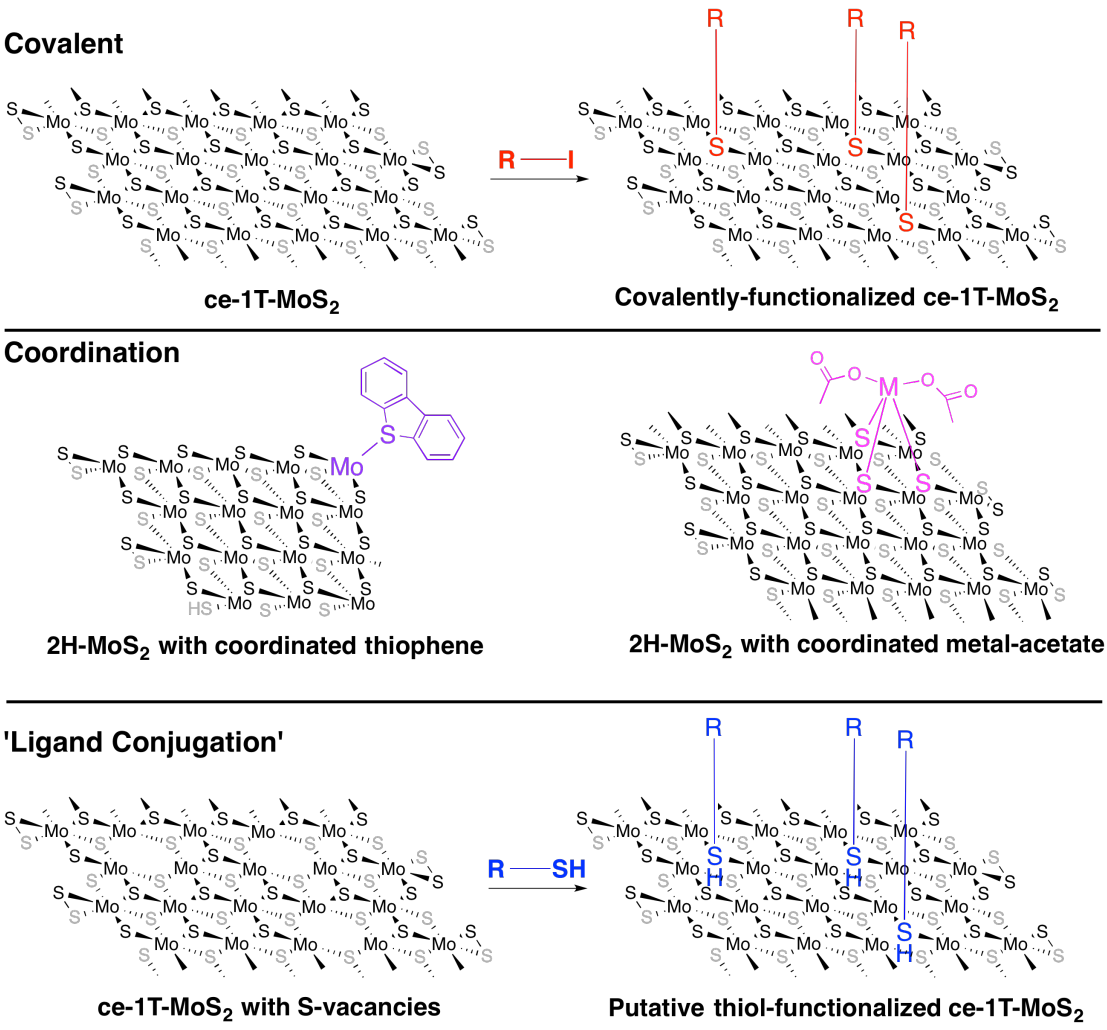

Figure 2. Graphical representations of various modes of MoS_2 functionalization with small molecules.

2.1 Covalent Functionalization of ce-1T-MoS_2.

Chemical exfoliation (ce) is a process where bulk 2H-MoS_2 is reacted with n-butyl lithium to yield the reduced product [Li_xMoS_2] (Scheme 1). This is then reacted with water (re-oxidized) causing delamination of MoS_2 monolayers and the formation of H_2 and LiOH.[32] This process yields MoS_2 that contains predominantly the 1T-polymorph (2H-MoS_2 also present), and thus we define the product as ce-1T-MoS_2. Methods employing ce-1T-MoS_2 have provided the only routes to covalently functionalized TMDs (Figure 2). The first example, by Chhowalla and co-workers,[33]

described the covalent functionalization of ce-1T-MoS_2, -WS_2, and -$MoSe_2$ nanosheets (Figures 2, 3) by reacting them with organoiodides (2-iodo-acetamide and iodomethane) or diazonium salts (also reported by Backes *et al*).[34] After preparing the ce-1T-TMD's in water, organoiodides were simply mixed into the aqueous dispersions and allowed to stir for 12 hours. X-ray photoelectron spectroscopy (XPS) analysis of the resulting functionalized materials gave no indication of remnant iodine atoms, suggesting functionalization through nucleophilic attack by ce-1T-MoS_2, causing displacement of iodide, had occurred. XPS analysis also confirmed the presence of N- and C-atoms on the ce-1T-MoS_2 surface (features in the N 1s and C 1s regions of the XPS spectrum). Importantly, the S 2p region showed the presence of new S-atoms on the ce-1T-MoS_2 surface, indicating the formation of a new C–S bond. Solid-state attenuated total reflectance Fourier transform infrared (ATR-FT-IR) and cross-polarization magic angle spinning (CP-MAS) NMR studies provided further support of the presence of organic functionalities on the ce-1T-MoS_2 surface. By ATR-FT-IR, a C–S vibration was observed at ν_{C-S} = 700 cm^{-1}, demonstrating the formation of a C–S bond. Critically, the ^{13}C CP-MAS NMR showed dramatic shifts in the resonances attributed to the organic functionalities compared to their precursors, providing strong evidence of a covalent tethering to the ce-1T-MoS_2. The loading of organic functionalities was estimated to be ~20% through both thermogravimetric analysis (TGA) and XPS analyses. This result is important, as the high degree of loading suggests functionalization occurred on the basal plane, and not just on the more reactive edge-sites. The study was extended to WS_2 and $MoSe_2$, yielding the same functionalization outcomes.

Monolayers of ce-1T-MoS_2 are normally not photoluminescent, unlike monolayers of

2H-MoS_2, however the covalently functionalized ce-1T-MoS_2 was photoluminescent. Another intriguing aspect of this work was that the functionalized ce-1T-MoS_2 could be converted to the semi-conducting polymorph 2H-MoS_2 through annealing at 300 °C. A 100% yield of 2H-MoS_2 was obtained, according to XPS, and the organic functionalities appeared to be intact, although the extremes of temperature are not suitable for most organic functional groups. This discovery is very important because 2H-MoS_2 does not react with organic iodides or diazonium salts, thus functionalization routes to the more attractive semi-conducting 2H-MoS_2 are limited.

Diazonium salts have been widely used to functionalize carbon-based nanomaterials including graphene and carbon nanotubes.[4] Backes and co-workers recently discovered that aryl-diazonium salts can be used for basal-plane functionalization of ce-1T-MoS_2.[34] ce-1T-MoS_2 was reacted with 4-methoxyphenyldiazonium tetrafluoroborate leading to an immediate flocculation of the nanosheets, indicating a change in the surface properties of the ce-1T-MoS_2. TGA of the functionalized ce-1T-MoS_2 showed a 7% weight loss in the temperature range 220-450 °C, suggesting the presence of organic guest molecules. TGA-coupled mass spectrometry (TGA-MS) verified that the weight loss during TGA heating originated from the organic functional groups (decay products of 4-methoxybenzene were detected). The degree of functionalization was considerably less than the 20% reported in the organoiodide Chemistry.[33] Backes et al prepared their ce-1T-MoS_2 in a slightly different fashion to Chhowalla, presumably leading to the lower degree of functionalization.

Importantly, a S–C vibrational mode was observed at ν_{C-S} = 695 cm^{-1} using FT-IR spectroscopy, indicating the formation of a C–S bond. Raman analysis showed that

the intensity ratio of the A_{1g} mode (404 cm^{-1}) to the 2LA(M) mode (450 cm^{-1}) was significantly higher in the functionalized sample compared to non-functionalized ce-1T-MoS_2 and pristine 2H-MoS_2. Backes proposed that this intensity ratio could be used as an indicator for the functionalization of MoS_2. Finally, XPS analysis of the functionalized ce-1T-MoS_2 provided some interesting insights. Firstly, the S 2p XPS spectra suggested the appearance of unique, non-MoS_2 sulfur species on the surface, demonstrating that a C–S bond had likely been formed. Secondly, the functionalized ce-1T-MoS_2 displayed enhanced stability (*i.e.* the 1T-polymorph did not isomerize to the 2H-polymorph) over long periods of times. This is unusual for ce-1T-MoS_2, because it normally isomerizes over a period of 1 week. Finally, the methoxybenzene-functionalized ce-1T-MoS_2 was re-dispersible in anisole, unsurprisingly, given the molecular similarities between methoxybenzene and anisole.

2.2 'Ligand Conjugation' Functionalization of ce-1T-MoS_2.

Dravid and co-workers reported the first example of an efficient functionalization of 2D TMDs (Figures 2, 3).[35] They reacted ce-1T-MoS_2 with bi-functional polyethyleneglycol (peg) molecules (one end of the polyether contained a thiol and the other end a hydroxyl, carboxylate, or ammonium functionality). Upon reaction between the ce-1T-MoS_2 and the organic thiol a marked change in the zeta-potential of the TMD nanosheets was observed, indicating a change in the ce-1T-MoS_2 surface properties. XPS analysis showed the presence of surface carbon and oxygen atoms, demonstrating the polyether functional groups were indeed bound to the surface of the ce-1T-MoS_2. Furthermore, FT-IR suggested that the thiol groups had reacted with the ce-1T-MoS_2, because the $\nu_{S\text{-}H}$ at 2563 cm^{-1} disappeared upon functionalization. The

disappearance of the thiol functionality would indicate it had reacted with the ce-1T-MoS_2. This observation was rather ambiguously described as the thiol being 'buried' within the ce-1T-MoS_2 surface.

The authors defined this functionalization technique as organic thiol 'ligand conjugation', although the exact nature of the thiol/MoS_2 interaction is unclear. It is possible that thiol ligands are coordinating to Mo-atoms in the ce-1T-MoS_2 at S-vacancies, yielding a 'ligand coordination' functionalization (Figure 2). This is how the functionalization was defined pictographically, although little experimental support for this postulate exists (*i.e.* XPS or FT-IR support for new/altered C–S or Mo–S bonds on the surface). As addressed in section 4, recent insights into the reaction between organic thiols and MoS_2 nanosheets appear to suggest the thiol functionality does not fill S-vacancies, but rather gets converted to a disulfide that is physisorbed on the MoS_2 surface.[36] Nonetheless, the 'ligand conjugated' ce-1T-MoS_2 functionalization method yielded ce-1T-MoS_2 nanosheets with interesting properties - the functionalized materials displayed extended coloidal stability compared to pristine ce-1T-MoS_2 (much like is observed when surfactants are used to exfoliate TMDs). Furthermore, the pegylated ce-1T-MoS_2 was an efficient host/support for certain biomolecules.

Li Zhou and colleagues subsequently used a similar procedure to functionalize ce-1T-MoS_2 with smaller, simpler organic thiols (Figure 3).[37] They coupled 1-mercaptopropionic acid, 1-thioglycerol, and L-cysteine to ce-1T-MoS_2 by reacting [Li_xMoS_2] (formed from the reaction between n-butyl lithium and 2H-MoS_2, Scheme 1) with the organic thiols dissolved in water. This method essentially mirrors Dravid's

method,[35] where the [Li_xMoS_2] was oxidized and exfoliated prior to reaction with the organic thiol. Presumably, concomitant exfoliation and functionalization occurred using Zhou's method of reacting the [Li_xMoS_2] with aqueous thiols. TGA analysis showed 6-9% loading of the organic functionalities, which were desorbed from the material in a rather large temperature range of 150 - 700 °C. XPS analyses showed the presence of organic C-, O- and N- atoms on the MoS_2 surface indicating the organic functional groups were interacting with the surface. Raman analysis of the functionalized 1T-MoS_2 was used to confirm surface modification - broadening of the A_{1g} and E^1_{2g} resonances was determined to derive from the presence of surface organic molecules. Unfortunately, the FT-IR analysis of the functionalized materials provided limited insight into the functional groups and their interaction with the ce-1T-MoS_2. For example, no $\nu_{C\text{-}S}$ was identified. One would expect this vibrational mode to shift dramatically if the organic thiol was coordinating to Mo-atoms at S-vacancies, and would thus provide definitive proof of ligand coordination to the nanomaterial surface. The exact nature of the ce-1T-MoS_2/organic thiol thus remains unclear.

Zhou's functionalized materials displayed exciting possibilities for the coupling of both inorganic and organic polymeric entities to ce-1T-MoS_2 nanosheets. The carboxylate-functionalized material supported the formation of discrete and well-defined silver nanoparticles on the ce-1T-MoS_2 surface, whereas the un-functionalized material yielded highly aggregated surface silver nanoparticles. The carboxylate-functionalized materials were also reacted with a polymethylmethacrylate precursor (hydroxylethyl methacrylate), which yielded a ce-1T-MoS_2 functionalized with ethyl methacrylate esters. Polymerization of these precursors yielded

polymethylmethacrylate (PMMA)-functionalized ce-1T-MoS_2. Along similar lines, the 1-thioglycerol-functionalized ce-1T-MoS_2 was reacted with caprolactone, yielding poly(caprolactone)-functionalized ce-1T-MoS_2. These examples represent some of the first examples of derivatization of functional groups on functionalized exfoliated ce-1T-MoS_2 and thus represent an important discovery.

Yuan Hu also employed the 'ligand conjugation' approach to functionalizing ce-1T-MoS_2 with silicates.[38] ce-1T-MoS_2 was reacted with dithioglycol using the Dravid method.[35] The authors propose that this functionalization method yields functionalized ce-1T-MoS_2 with hanging thiol groups, in which one thiol of the dithioglycol reacted with the ce-1T-MoS_2, while the other did not. No evidence to support this postulate was provided. The dithioglycol-functionalized ce-1T-MoS_2 was then reacted with octavinyl polyhedral oligomeric silsequioxanes (OvlPOSS) presumably through thiol-ene chemistry to give OvlPOSS-functionalized ce-1T-MoS_2. This material was then coated with polyvinyl alcohol (PVA). FT-IR analysis of the final material showed the presence of Si–O–Si vibrational modes, confirming the presence of surface silsequioxanes. Unfortunately, no insight into the thiol/MoS_2 interaction, or indeed the thiol-ene reaction was provided. The OvlPOSS-MoS_2-PVA displayed improved thermal oxidative resistance when tested as a flame-retardant material.

Cai, Liu, and co-workers reported the preparation of iron oxide decorated ce-1T-MoS_2 nanosheets employing the 'ligand conjugation' technique.[39] In this instance, meso-2,3-dimercaptosuccinic acid (Figure 3) coated iron oxide nanoparticles were reacted with ce-1T-MoS_2 using the Dravid method.[35] It was postulated that the dithiol of the

meso-2,3-dimercaptosuccinic acid was filling S-atom vacancies on the ce-1T-MoS_2 surface, however as with the other 'ligand conjugation' methods no evidence to support this postulate was provided. The iron-oxide decorated ce-1T-MoS_2 was then further coated with polyethylene glycol to make the nanomaterials stable under physiological conditions. ^{64}Cu ions could be stably adsorbed to the resulting nanoparticles allowing for the application of these materials in photothermal therapeutics.

In a particularly interesting slant on the thiol 'ligand conjugation' theme, Liu *et al* reacted ce-1T-MoS_2 with an organic disulfide containing substrate, pegylated lipoic acid (Figure 3).[40] They postulated that sulfur atoms in the lipoic acid would fill S-atom vacancies. Unfortunately very little investigation into the atomic level interaction of the lipoic acid with ce-1T-MoS_2 was provided. Certainly the pegylated lipoic acid sticks to the ce-1T-MoS_2, greatly enhancing its dispersibility in aqueous media, while the UV-vis absorption properties of the functionalized material do not change when compared to pristine ce-1T-MoS_2. Of particular interest from a reactivity perspective however, is the reaction between the disulfide lipoic acid and 1T-ce-MoS_2. It is possible that rather than 'ligand conjugation' being the mode of binding with ce-1T-MoS_2, that in fact a covalent disulfide bond, as a result of radical coupling, had formed between a S-atom of the MoS_2 and an S-atom from the organic disulfide.

3. Functionalization of 2H-MoS_2

Besenbacher and co-workers produced a fascinating set of results on chemical vapor

deposition (CVD) synthesized 2H-MoS_2 monolayered nanoparticles (Figures 2, 3).[41] They demonstrated the preparation of an array of MoS_2 clusters of varying size (from 3 Mo- and 7 S-atoms up to 36 Mo- and 102 S-atoms). These particles display varying degrees of S-atom vacancies as evidenced by scanning tunneling microscopy (STM) analysis. Amazingly, STM analysis showed that dibenzothiophene interacted with the MoS_2 nanoparticles, with the S-atom of the dibenzothiophene filling an S-atom vacancy (Figure 2). This would suggest that the S-atom of dibenzothiophene coordinated (formed a dative bond) to the Mo-atom at an S-atom vacancy. The coordination site was quite open, at a corner site on a triangular particle, presumably providing sufficient space for the thioether ligand to access the Mo- atom in order to coordinate. Interestingly, no examples of the thioether ligand interacting with basal plane or edge sites were reported, suggesting the availability of corner sites is essential for S-atom containing molecules to interact with MoS_2 at S-atom vacancies.

Li and co-workers later took advantage of this functionalization technique by reacting thionine (3,7-diamino-5-phenothiazinium acetate), a molecular analogue of dibenzothiophene, with liquid exfoliated 2H-MoS_2 in the presence of an ionic liquid.[42] XPS analysis added critical weight to the observations of Besenbacher, because it provided conclusive proof that a new S 2p feature was present in the thionine-functionalized materials. Importantly, this new feature was distinctly different to S 2p features observed for pristine 2H-MoS_2 *and* thionine. This strongly indicates the formation of a S–Mo or S–S bond between thionine and MoS_2. Besenbacher's observations would suggest that this was a dative bond. The thionine-functionalized 2H-MoS_2 was used to detect DNA, displaying a decreased electrochemical response in the presence of DNA at very low concentrations,

allowing for the efficient detection of DNA in highly dilute samples.

The McDonald lab reported one of the first examples of functionalization of 2H-MoS_2.[43] Coordination (formation of a dative bond) by basal plane S-atoms to metal salts yielded functionalized 2H-MoS_2 (Figures 2, 3). Liquid exfoliated 2H-MoS_2 dispersed in iso-propanol was reacted with metal-acetate salts ($M(OAc)_2$; M = Ni, Cu, Zn). X-ray photoelectron spectroscopy (XPS) analysis suggested that coordination of surface S-atoms to the $M(OAc)_2$ had occurred, as evidenced by the appearance of new S 2p features in the XPS core level spectra of the functionalized materials. Diffuse reflectance infrared Fourier transform (DRIFT) spectroscopy showed the presence of surface carboxylate vibrational modes that were shifted with respect to the $M(OAc)_2$ precursors, indicating coordination of surface S-atoms to the metal center. TGA showed the presence of organic functionalities that combusted at approximately 200 °C, while post-TGA DRIFT analysis showed the loss of the carboxylate stretching modes. Most interestingly, functionalization of the 2H-MoS_2 allowed for its dispersion/processing in more conventional lab solvents including acetone, rather than the highly toxic solvent N-methyl-2-pyrrolidone (NMP), which is normally used to disperse 2H-MoS_2. This coordination method is extremely facile and highly efficient, however it does not yield covalently or tightly-bound functionalized 2H-MoS_2, with the functionalities rather easily removed through multiple washings with NMP.

Leite and co-workers took an alternative approach to functionalizing 2H-MoS_2 in what they describe as a covalent manner.[44] Liquid exfoliated 2H-MoS_2 (NMP as exfoliating solvent) was mixed with polybutadiene in toluene/NMP over a period of six days. The resulting functionalized 2H-MoS_2 displayed greatly enhanced

dispersibility in pure toluene, providing a strong indication of a change in the surface properties of the 2H-MoS_2. Transmission electron microscopy (TEM) provided evidence that the organic polymer was bound to the 2H-MoS_2 surface with an organic layer thickness of ~30 nm. The authors suggested that the TEM indicated the presence of a C–S bond at the interface between the polymer and 2H-MoS_2, however, the resolution is such that this postulate cannot be confirmed. XPS analysis of the polybutadiene functionalized 2H-MoS_2 showed the Mo- and S-atoms remained in the same chemical state as before functionalization, indicating that the PB/MoS_2 interaction was not covalent. FT-IR analysis showed the presence of a putative C–S vibrational mode (at a very low 630 cm^{-1}), providing support for their postulate that the functionalization was covalent. Interestingly, the functionalization appears to have occurred only at the disulfide-rich edge sites on the 2H-MoS_2 (according to TEM). This would suggest that the disulfide edge groups have attacked the polybutadiene alkene. Further investigations into the nature of the polybutadiene/2H-MoS_2 interaction are warranted, as this would represent the only example of covalent functionalization of 2H-MoS_2. Although the functionalization occurs at edge sites, and not the basal plane, it represents an important breakthrough.

In an interesting, alternative, application of the thiol 'ligand conjugation' studies, two groups have used organic thiols as S-atom donors. S-atoms from these thiols were used to fill S-atom vacancies in 2H-MoS_2 monolayers, with the elimination of the remaining organic fragment. Makarova and Okawa reported that dodecanethiol or (3-mercaptopropyl)-trimethoxysilane molecules (Figure 3) could coat a 2H-MoS_2 surface as evidenced by STM analysis.[45] Furthermore, they found that the STM tip could induce S-atom vacancy repairs in the presence of the dodecanethiol. In a similar

(later) report Yu and Pan showed that by coating 2H-MoS_2 with (3-mercaptopropyl)-trimethoxysilane and then annealing (350 °C) the resulting material in the presence of H_2, S-atom vacancies in the 2H-MoS_2 monolayers were repaired .[46] The exact nature of the S-atom donation is not clear - it would require an unusual C–S bond scission step and the formation of organic by-products. Yu and Pan propose that initial coordination of the thiol ligand at S-atom vacancies precedes C–S bond scission. Unfortunately, the STM and high-resolution TEM images displayed in these reports cannot confirm this postulate. The extremes of condition (the STM tip or annealing at 350 °C in the presence of H_2) could facilitate the C–S bond breakage, however how the S-atom occupies S-atom vacancies prior to this is difficult to predict. Overall, however, these reports demonstrate a simple approach to developing pristine monolayers of 2H-MoS_2 from defect-rich materials.

Daenecke recently reported the functionalization of 2H-MoS_2 through reaction with organic thiols (4-mercaptophenol, thiophenol, 1-propanethiol, 1-nonanethiol, and 1-dodecanethiol, Figure 3) in a fashion similar to Dravid's 'ligand conjugation' method.[47] 2H-MoS_2 was exfoliated by grinding and subsequent ultra-sonication in ethanol. The exfoliated materials were stirred with a large excess of thiol over a 24 h period followed by dialysis in ethanol/water for a further 24h. As in the 'ligand conjugation' Chemistry, Daenecke noted the disappearance of thiol S-H ($\nu_{S\text{-}H}$ ~ 2500 cm^{-1}) vibrational modes in the ATR-FT-IR spectra of the functionalized materials. Interestingly, a comparison of the ATR-FT-IR spectra of the free thiols and the functionalized materials indicates minor chemical changes to the properties of the thiol groups tethered to the 2H-MoS_2. The photoluminescence spectra of the functionalized 2H-MoS_2 displayed slightly red-shifted emissions compared to pristine

2H-MoS_2, putatively as a result of the functionalities on the surface tuning the emission. Unfortunately, very little insight into the nature of the organic thiol/2H-MoS_2 interaction was provided (*i.e.* XPS, Raman, CP-MAS NMR), and thus there is insufficient support for the postulate that this is a covalent tethering.

Jung reported a similar approach to functionalizing 2H-MoS_2 with mercaptoundecanoic acid (Figure 3).[48] As in previous reports on the reaction between thiols and MoS_2, no thiol S-H ($\nu_{S\text{-}H} \sim 2540\ cm^{-1}$) vibrational modes were observed in the functionalized material, indicating the organic thiol had reacted. FT-IR analysis did show the presence of surface aliphatic and carbonyl groups. XPS analysis also confirmed the presence of organic groups on the 2H-MoS_2 surface, however, did not provide insight into the nature of the thiol/2H-MoS_2 interaction (*i.e.* no comparison of the thiol XPS versus the thiol functionalized 2H-MoS_2 was provided). Lee and coworkers later used the same protocols to prepare alkane-thiol functionalized 2H-MoS_2.[49] The resulting materials were probed electrochemically. Lee postulated that vacancies in the 2H-MoS_2 were 'passivated' by the organic thiols, although limited support for this postulate was provided. The functionalized nanomaterials did indeed display different physical properties compared to pristine 2H-MoS_2, however, the exact nature of the organic thiol/2H-MoS_2 interaction had not been probed sufficiently.

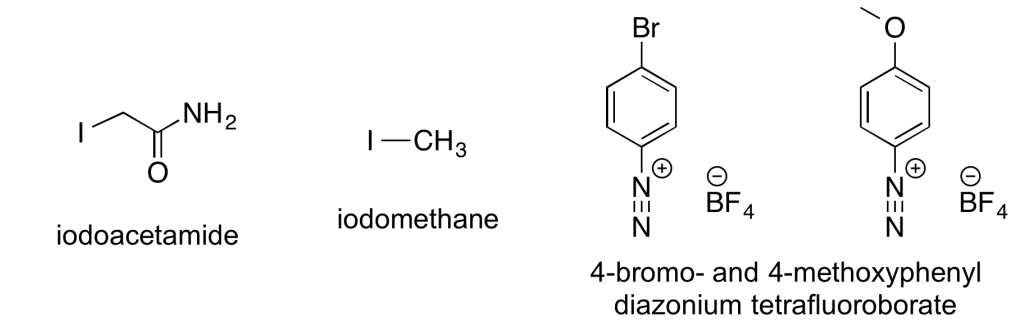

Figure 3. Organic/inorganic compounds for the functionalization of TMDs.

4. Discussion and Conclusions.

The past 2-3 years has seen great developments in the field of 2D TMD functionalization. Herein we have reviewed techniques towards the chemical functionalization of TMDs, *i.e.* approaches that lead to a bond linking TMD and functionality (Figure 2). The covalent functionalization Chemistry of Chhowalla and Backes represents the only well-characterized examples of covalent tethering of organic functionalities to TMDs. All other examples described above are either non-covalent or have not provided sufficient proof to show the functionalization leads to bond formation. TMDs have shown a propensity to being very sticky - many organic groups will physisorb on the TMDs, likely through electrostatic interactions with the electron-rich chalcogen surface atoms. It is therefore important that techniques including FT-IR, CP-MAS NMR, and XPS spectroscopies are employed to prove the existence of a TMD-to-functionality bond (*e.g.* new C–S or new Mo–S bonds in functionalized MoS_2).

The excellent covalent tethering efforts of Chhowalla and Backes lead one to consider the bonding in covalently functionalized TMD monolayers. For example, how is the C–S bond formed in the reaction between TMD chalcogen atom and organic electrophile? Backes postulated that the ce-1T-MoS_2 contains remnant negative charge (*i.e.* MoS_2 in a partially reduced state, $Li_x[MoS_2]^{x-}$) that was not quenched in the delamination step (Scheme 1). This remnant surface charge was believed to nucleophilically attack the electrophilic carbon of the diazonium salt. This postulate is plausible, but requires further verification: pristine (charge-free) 1T-MoS_2 should be

reacted with diazonium salts, if it does not yield C–S bond formation, the postulate is likely correct. An alternative theory is that 1T-MoS_2 is inherently unstable, causing the bridging sulfide atoms to be good nucleophiles *or* just susceptible to electrophiles. Clearly ce-1T-MoS_2 is indeed highly activated compared to 2H-MoS_2 which does not react with any of the above-mentioned electrophiles. The structure of 1T-MoS_2 is poorly understood. It is believed to be quite distorted compared to that of 2H-MoS_2 , which could cause it to be very reactive.[15, 32] Given our poor understanding of the structure of 1T-MoS_2 it is not yet possible to definitively explain why and how it reacts with electrophiles.

A second point of consideration is that the covalently bound organic functional groups are going to weaken the Mo–S bonds in ce-1T-MoS_2, and thus dramatically alter the structural and electronic properties of the TMD. Changes in the electronic properties are evident in the unexpected photoluminescence in functionalized ce-1T-MoS_2 (that is absent in un-functionalized ce-1T-MoS_2). However, more analysis of the structural integrity of the functionalized monolayers is desirable in order to fully understand the effect of introducing organic functional groups through covalent C–S bonds on the surface of MoS_2 monolayers. Finally, although these functionalization methods yield covalently functionalized ce-1T-MoS_2 that can be isomerized to 2H-MoS_2 by annealing at 300 °C, an alternative route to covalently functionalized 2H-MoS_2 is much sought after, because not many organic or bio-molecules will survive such extremes of temperature.

As described in sections 2 and 3 there are now many examples of organic thiols reacting with MoS_2 yielding functionalized MoS_2. This functionalization technique

has been described as a bond-forming or covalent functionalization method, *i.e.* a Mo–S bond between an S-atom in the organic functional group and a Mo-atom in the MoS_2 has been formed. This conclusion is drawn from infra-red spectroscopy that shows the loss of S–H vibrational modes after the MoS_2 reacted with the thiol. Unfortunately, these studies have not provided sufficient further experimental support for this 'bonding' description to be attributed. In a very recent set of experiments,[36] we demonstrated a general route to functionalize 2H-MoS_2 with cysteine (an organic thiol). Critically, MoS_2 was found to be facilitating the oxidation of the thiol, cysteine, to the disulfide, cystine, during functionalization (accounting for the loss of the S–H FT-IR peaks). The resulting cystine was physisorbed on MoS_2 rather than any bond-forming process having occurred. These observations were found to be true for other organic thiols and indeed other TMDs. Our findings suggest that functionalization of 2D MoS_2 using organic thiols does not yield covalently or datively bonded functionalities. Future efforts in the 'ligand conjugation' area thus need to provide more insight into the interaction between organic thiols and MoS_2.

To date, functionalization of TMDs has focused on the functionalization reactivity of the material - thus *how* do we functionalize? The reports of the last 2-3 years have provided multiple routes to functionalize 2D TMDs, although some of these methods require further exploration. An array of molecules react with or physisorb to MoS_2, leading to functionalization of the material (Figure 3). The coming years should address *what* functionalization can facilitate: Can we produce large quantities of monolayers of TMDs through functionalization? Can we tune the electronic properties of TMDs through functionalization? Using functionalization can we couple TMDs with other materials to develop multifunctional devices? Ultimately, having addressed

these questions, we expect the exploitation of the functionalization of TMDs will contribute to the widespread application of TMDs in photonics, energy storage and conversion, drug delivery and medical devices.

Acknowledgements:

Research in the McDonald lab is supported by the European Union (FP7-333948) and a research grant from Science Foundation Ireland (SFI/12/RC/2278).

References:

[1] K. S. Novoselov, A. K. Geim, S. V. Morozov, D. Jiang, Y. Zhang, S. V. Dubonos, I. V. Grigorieva, A. A. Firsov, *Science* **2004**, *306*, 666-669.
[2] A. K. Geim, K. S. Novoselov, *Nat. Mater.* **2007**, *6*, 183-191.
[3] M. J. Allen, V. C. Tung, R. B. Kaner, *Chem. Rev.* **2010**, *110*, 132-145.
[4] V. Georgakilas, M. Otyepka, A. B. Bourlinos, V. Chandra, N. Kim, K. C. Kemp, P. Hobza, R. Zboril, K. S. Kim, *Chem. Rev.* **2012**, *112*, 6156-6214.
[5] J. N. Coleman, *Acc. Chem. Res.* **2013**, *46*, 14-22.
[6] S. Z. Butler, S. M. Hollen, L. Cao, Y. Cui, J. A. Gupta, H. R. Gutierrez, T. F. Heinz, S. S. Hong, J. Huang, A. F. Ismach, E. Johnston-Halperin, M. Kuno, V. V. Plashnitsa, R. D. Robinson, R. S. Ruoff, S. Salahuddin, J. Shan, L. Shi, M. G. Spencer, M. Terrones, W. Windl, J. E. Goldberger, *ACS Nano* **2013**, *7*, 2898-2926.
[7] C. N. R. Rao, H. S. S. Ramakrishna Matte, U. Maitra, *Angew. Chem. Int. Ed.* **2013**, *52*, 13162-13185.
[8] V. Nicolosi, M. Chhowalla, M. G. Kanatzidis, M. S. Strano, J. N. Coleman, *Science* **2013**, *340*, 1420-+.
[9] M. Xu, T. Liang, M. Shi, H. Chen, *Chem. Rev.* **2013**, *113*, 3766–3798.
[10] P. Miro, M. Audiffred, T. Heine, *Chem. Soc. Rev.* **2014**, *43*, 6537-6554.
[11] R. Lv, J. A. Robinson, R. E. Schaak, D. Sun, Y. Sun, T. E. Mallouk, M. Terrones, *Acc. Chem. Res.* **2015**, *48*, 56-64.
[12] M. Chhowalla, H. S. Shin, G. Eda, L.-J. Li, K. P. Loh, H. Zhang, *Nat. Chem.* **2013**, *5*, 263-275.
[13] L. F. Mattheiss, *Phys. Rev. B* **1973**, *8*, 3719-3740.
[14] P. D. Fleischauer, J. R. Lince, P. A. Bertrand, R. Bauer, *Langmuir* **1989**, *5*, 1009-1015.
[15] M. Kan, J. Y. Wang, X. W. Li, S. H. Zhang, Y. W. Li, Y. Kawazoe, Q. Sun, P. Jena, *J. Phys. Chem. C* **2014**, *118*, 1515-1522.
[16] B. Schonfeld, J. J. Huang, S. C. Moss, *Acta Cryst. B* **1983**, *39*, 404-407.
[17] K. S. Novoselov, D. Jiang, F. Schedin, T. J. Booth, V. V. Khotkevich, S. V. Morozov, A. K. Geim, *Proc. Natl. Acad. Sci.* **2005**, *102*, 10451-10453.
[18] J. N. Coleman, M. Lotya, A. O'Neill, S. D. Bergin, P. J. King, U. Khan, K. Young, A. Gaucher, S. De, R. J. Smith, I. V. Shvets, S. K. Arora, G. Stanton, H.-Y. Kim, K. Lee, G. T. Kim, G. S. Duesberg, T. Hallam, J. J. Boland, J. J. Wang, J. F. Donegan, J. C. Grunlan, G. Moriarty, A. Shmeliov, R. J. Nicholls, J. M. Perkins, E. M. Grieveson, K. Theuwissen, D. W. McComb, P. D. Nellist, V. Nicolosi, *Science* **2011**, *331*, 568-571.
[19] R. J. Smith, P. J. King, M. Lotya, C. Wirtz, U. Khan, S. De, A. O'Neill, G. S. Duesberg, J. C. Grunlan, G. Moriarty, J. Chen, J. Wang, A. I. Minett, V. Nicolosi, J. N. Coleman, *Adv. Mat.* **2011**, *23*, 3944-3948.
[20] Z. Zeng, Z. Yin, X. Huang, H. Li, Q. He, G. Lu, F. Boey, H. Zhang, *Angew. Chem. Int. Ed.* **2011**, *50*, 11093-11097.
[21] K.-K. Liu, W. Zhang, Y.-H. Lee, Y.-C. Lin, M.-T. Chang, C.-Y. Su, C.-S. Chang, H. Li, Y. Shi,

H. Zhang, C.-S. Lai, L.-J. Li, *Nano Lett.* **2012**, *12*, 1538-1544.
[22] L. Niu, K. Li, H. Zhen, Y.-S. Chui, W. Zhang, F. Yan, Z. Zheng, *Small* **2014**, *10*, 4651-4657.
[23] S. Presolski, M. Pumera, *Mater. Today* **2015**, doi:10.1016/j.mattod.2015.08.019
[24] W. Yin, L. Yan, J. Yu, G. Tian, L. Zhou, X. Zheng, X. Zhang, Y. Yong, J. Li, Z. Gu, Y. Zhao, *ACS Nano* **2014**, *8*, 6922-6933.
[25] B. L. Li, H. Q. Luo, J. L. Lei, N. B. Li, *RSC Adv.* **2014**, *4*, 24256-24262.
[26] P. Joo, K. Jo, G. Ahn, D. Voiry, H. Y. Jeong, S. Ryu, M. Chhowalla, B.-S. Kim, *Nano Lett.* **2014**, *14*, 6456-6462.
[27] M. A. Hussain, M. Yang, T. J. Lee, J. W. Kim, B. G. Choi, *J. Colloid Interface Sci.* **2015**, *451*, 216-220.
[28] W. Zhang, Y. Wang, D. Zhang, S. Yu, W. Zhu, J. Wang, F. Zheng, S. Wang, J. Wang, *Nanoscale* **2015**, *7*, 10210-10217.
[29] S. S. Chou, Y.-K. Huang, J. Kim, B. Kaehr, B. M. Foley, P. Lu, C. Dykstra, P. E. Hopkins, C. J. Brinker, J. Huang, V. P. Dravid, *J. Am. Chem. Soc.* **2015**, *137*, 1742-1745.
[30] R.-M. Kong, L. Ding, Z. Wang, J. You, F. Qu, *Anal. Bioanal. Chem.* **2015**, *407*, 369-377.
[31] L. David, R. Bhandavat, U. Barrera, G. Singh, *Sci. Rep.* **2015**, *5*, 9792.
[32] E. Benavente, M. A. Santa Ana, F. Mendizábal, G. González, *Coord. Chem. Rev.* **2002**, *224*, 87-109.
[33] D. Voiry, A. Goswami, R. Kappera, C. d. C. C. e. Silva, D. Kaplan, T. Fujita, M. Chen, T. Asefa, M. Chhowalla, *Nat. Chem.* **2015**, *7*, 45-49.
[34] K. C. Knirsch, N. C. Berner, H. C. Nerl, C. S. Cucinotta, Z. Gholamvand, N. McEvoy, Z. Wang, I. Abramovic, P. Vecera, M. Halik, S. Sanvito, G. S. Duesberg, V. Nicolosi, F. Hauke, A. Hirsch, J. N. Coleman, C. Backes, *ACS Nano* **2015**, *9*, 6018-6030.
[35] S. S. Chou, M. De, J. Kim, S. Byun, C. Dykstra, J. Yu, J. Huang, V. P. Dravid, *J. Am. Chem. Soc.* **2013**, *135*, 4584–4587.
[36] X. Chen, N. C. Berner, C. Backes, G. S. Duesberg, A. R. McDonald, submitted **2015**.
[37] Z. Cheng, B. He, L. Zhou, *J. Mater. Chem. A* **2015**, *3*, 1042-1048.
[38] S.-D. Jiang, G. Tang, Z.-M. Bai, Y.-Y. Wang, Y. Hu, L. Song, *RSC Adv.* **2014**, *4*, 3253-3262.
[39] T. Liu, S. Shi, C. Liang, S. Shen, L. Cheng, C. Wang, X. Song, S. Goel, T. E. Barnhart, W. Cai, Z. Liu, *ACS Nano* **2015**, *9*, 950-960.
[40] T. Liu, C. Wang, X. Gu, H. Gong, L. Cheng, X. Shi, L. Feng, B. Sun, Z. Liu, *Adv. Mater.* **2014**, *26*, 3433-3440.
[41] A. Tuxen, J. Kibsgaard, H. Gøbel, E. Lægsgaard, H. Topsøe, J. V. Lauritsen, F. Besenbacher, *ACS Nano* **2010**, *4*, 4677-4682.
[42] T. Wang, R. Zhu, J. Zhuo, Z. Zhu, Y. Shao, M. Li, *Anal. Chem.* **2014**, *86*, 12064-12069.
[43] C. Backes, N. C. Berner, X. Chen, P. Lafargue, P. La Place, M. Freeley, G. S. Duesberg, J. N. Coleman, A. R. McDonald, *Angew. Chem. Int. Ed.* **2015**, *54*, 2638-2642.
[44] R. H. Goncalves, R. Fiel, M. R. S. Soares, W. H. Schreiner, C. M. P. Silva, E. R. Leite, *Chem. - Eur. J.* **2015**, 21, 15583–15588.
[45] M. Makarova, Y. Okawa, M. Aono, *J. Phys. Chem. C* **2012**, *116*, 22411-22416.
[46] Z. Yu, Y. Pan, Y. Shen, Z. Wang, Z.-Y. Ong, T. Xu, R. Xin, L. Pan, B. Wang, L. Sun, J. Wang, G. Zhang, Y. W. Zhang, Y. Shi, X. Wang, *Nat. Commun.* **2014**, *5*.
[47] E. P. Nguyen, B. J. Carey, J. Z. Ou, J. van Embden, E. D. Gaspera, A. F. Chrimes, M. J. S. Spencer, S. Zhuiykov, K. Kalantar-zadeh, T. Daeneke, *Adv. Mater.* **2015**, 27, 6225–6229.
[48] J.-S. Kim, H.-W. Yoo, H. O. Choi, H.-T. Jung, *Nano Lett.* **2014**, *14*, 5941-5947.
[49] K. Cho, M. Min, T.-Y. Kim, H. Jeong, J. Pak, J.-K. Kim, J. Jang, S. J. Yun, Y. H. Lee, W.-K. Hong, T. Lee, *ACS Nano* **2015**, *9*, 8044-8053.